Optical properties of the alkali-metal-doped superconducting fullerenes: K_3C_{60} and Rb_3C_{60}

L. Degiorgi
Laboratorium für Festkörperphysik, Eidgenössische Technische Hochschule Zürich, CH-8093 Zürich, Switzerland

E. J. Nicol
Department of Physics, University of California at Santa Barbara, Santa Barbara, California 93106

O. Klein* and G. Grüner
Department of Physics and Solid State Science Center, University of California at Los Angeles, Los Angeles, California 90024

P. Wachter
Laboratorium für Festkörperphysik, Eidgenössische Technische Hochschule Zürich, CH-8093 Zürich, Switzerland

S.-M. Huang, J. Wiley, and R. B. Kaner
Department of Chemistry and Biochemistry and Solid State Science Center, University of California at Los Angeles, Los Angeles, California 90024

(Received 20 September 1993; revised manuscript received 18 November 1993)

We have measured the optical reflectivity over a broad spectral range of single-phase K_3C_{60} and Rb_3C_{60} compounds, and have evaluated the optical conductivity both below and above the superconducting transition temperature. We identify various features in the excitation spectrum of the normal state: a Drude contribution at low frequency, a midinfrared absorption, and several interband transitions. In the superconducting state our results are in full agreement with a BCS singlet ground state, with the measured gap values consistent with the weak-coupling limit. We also evaluate several intrinsic parameters characterizing both the normal and superconducting state, such as the plasma frequency, the relaxation scattering rate, and the mean free path, besides the superconducting gaps and the penetration depth. We compare these quantities with similar ones from other experiments and find satisfactory agreement. Moreover, we present our calculation of the electrodynamic response above and below T_c with the standard Eliashberg electron-phonon theory of superconductivity, which strongly supports a pairing mechanism mediated by high-frequency intramolecular phonon modes.

I. INTRODUCTION

The discovery[1,2] of superconductivity at relatively high temperatures in the alkali-metal C_{60} compounds has created considerable interest. Despite a variety of experiments, several issues remain controversial either for the normal- or for the superconducting-state properties. The central question, of course, is about the nature of the pairing mechanism. There has been debate about whether electron-electron[3] interactions on the C_{60} ball or electron-phonon (e-ph) coupling[4–6] mediate the pairing. Concerning the latter mechanism, there is still quite a bit of controversy with respect to arguments, favoring electron-phonon interactions with *low*-frequency *inter*molecular vibrations[6] or with *high*-frequency *intra*molecular modes.[4,5]

The energy scale of the various modes which mediate the e-ph coupling are different, and therefore, which of these are important, could, in principle, be decided by examining whether the weak- or strong-coupling limit applies. In the case of high-frequency phonons for example, one expects, within the mean-field BCS theory, the weak-coupling limit to be appropriate with the ratio of the single-particle gap Δ and the transition temperature T_c given by $2\Delta/k_BT_c=3.52$. In the case of low-frequency vibrations, on the other hand, $2\Delta/k_BT_c$ is expected to exceed the value which is appropriate for the weak-coupling limit.

In this context, the optical investigation, besides characterizing the normal-state properties, is also a powerful experimental tool in order to single out whether the weak- or strong-coupling limit of the BCS theory is more appropriate to describe the superconducting state. The first available experiments on these issues led to different values of the single-particle gap in K_3C_{60} and Rb_3C_{60} compounds. Tunneling measurements[7] on Rb_3C_{60} place the single-particle gap well into the strong-coupling limit with $2\Delta/k_BT_c\approx5$. Optical experiments on both compounds, which are based only on the ratio of the normal- and superconducting-state reflectivities R_s/R_n or transmissions T_s/T_n, either claim to observe the weak-coupling limit[8] or to reflect a distribution of superconducting gaps.[9] The reasons for these differences are not understood at present.

In this paper we review our (absolute) optical reflectivity measurements on single-phase K_3C_{60} and Rb_3C_{60}. From the discussion of the complete excitation spectrum, extending from the far infrared (FIR) up to the

visible and ultraviolet (UV) frequency range, we evaluate several intrinsic parameters, characterizing the normal- and superconducting-state properties. Particularly, our reflectivity measurements show clear evidence of well defined superconducting gaps with $2\Delta/k_BT_c$ in full agreement with the prediction of the weak-coupling BCS limit. Moreover, by applying a sum rule argument we extrapolate the plasma frequency associated with the free charge carriers in the normal state and the penetration depth for the superconducting state.

Our paper is organized as follows: In Sec. II we describe the experimental technique, characterize our specimens, and also present the experimental results. In Sec. III we discuss our experimental findings, comparing the intrinsic parameters evaluated from our optical investigations (both above and below T_c) with similar quantities arrived at from other experiments. Furthermore, the implications of our results relative to different theoretical approaches will be discussed. In this respect, we also present our theoretical analysis, based on the Eliashberg formalism. Finally, in Sec. IV, we summarize our main experimental findings pointing out, however, those controversial and puzzling problems which still need further investigations to be solved. Part of this work has been published elsewhere.[10,11]

II. EXPERIMENT AND RESULTS

The K_3C_{60} and Rb_3C_{60} specimens were prepared by a gas-solid reaction between C_{60} and gaseous alkali metal, in a way similar to that reported earlier.[1,2] Indeed, C_{60} and potassium (Alfa, 99.95%) or rubidium (Mackay, high purity) were loaded into a flame-dried Pyrex tube in a helium-filled drybox. To make manipulation of the alkali metal easier and to only allow the pure gas-phase material to come in contact with the fullerene, the metal was weighted out on a small piece of glass and this combination was placed in the tube with C_{60}. The tube was sealed under vacuum ($\sim 10^{-6}$ Torr). The reaction vessel was placed in a furnace with the C_{60} and the metal positioned at opposite ends of the tube. The sample was heated at 200 °C until all of the metal was consumed by the fullerene (typically two days). Samples were then transferred to Pyrex x-ray capillaries. Heat treatment was continued at 200 °C until no further change in the x-ray diamagnetism could be observed: typically one week for the potassium samples and five weeks for the rubidium samples. The procedure led to a fractional shielding diamagnetism of about 40–50 % for both K and Rb powder samples, determined relative to a Nb bulk reference sample. The reduced Meissner fraction is most probably due to the fine powder used with the grain size comparable to the penetration depth. The samples have a superconducting phase transition temperature $T_c = 29$ K and 19 K for the Rb- and K-fullerene, respectively. The powder was then pressed in a He chamber in order to obtain pellet of about 3 mm diam and 1 mm thick, and sealed in a glass capillary with He atmosphere.

Figure 1 displays the measurement of the temperature dependence of the resistivity of K_3C_{60} using a contactless technique.[12] An especially prepared pressed pellet (8 mm diam and 1 mm thick) of K_3C_{60} forms one wall of a cylindrical cavity, resonating in the TE_{011} mode at microwave frequency of 60 GHz (2 cm^{-1}). By measuring the temperature dependence of the bandwidth and the characteristic frequency of the resonator we can evaluate the electrical properties of the sample.[12] In Fig. 1 two measurements are displayed, where in the second run (open circles) we have reground the sample and repressed it following the same procedure as for the first preparation. Our results are in contrast with the upturn to higher resistivity with decreasing temperature observed in $\rho(T)$ for thin films[13] but in qualitative agreement with earlier results on single crystals.[14] The granularity of the thin films is most probably the reason for the discrepancy. Nevertheless, it should be noted that we observe a much stronger temperature dependence (the resistivity drops by almost an order of magnitude between 300 and 20 K, where at the transition temperature $\rho(20\ \text{K}) = 0.5$ mΩ cm) than $\rho(T)$ observed in single crystals.[14] Furthermore, the temperature dependence of the resistivity can be fitted by the functional form $\rho(T) = a + bT^2$.[12]

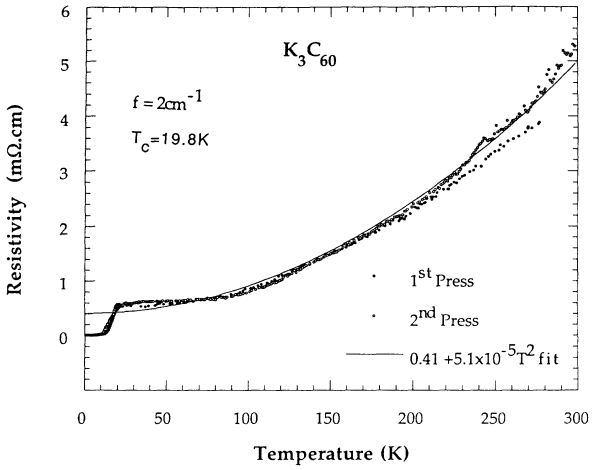

FIG. 1. Temperature dependence of the intrinsic resistivity of K_3C_{60}. The solid line represents a fit of the data using the functional form $\rho(T) = a + bT^2$.

Reflectivity measurements $[R(\nu)]$ were performed between 14 and 50 000 cm^{-1} using three different spectrometers. In the far-infrared (FIR) spectral range we measured $R(\nu)$ also as function of the temperature. The photon energy range between 14 and 800 cm^{-1} was covered with a Bruker IFS 113v Fourier Interferometer with a Hg arc light source and He-cooled silicon bolometer detector. From the FIR up to mid-IR a fast scanning Bruker interferometer IFS 48PC was used, while in the visible spectral range a homemade spectrometer based on a Zeiss monochromator was employed. A gold mirror was used as reference in the FIR and mid-IR. After all measurements have been performed, the pellets were covered with a 400-Å layer of gold in order to take into account the surface roughness (particularly important here, since the

pellet cannot be polished). No smoothing of the spectra has been performed, since the signal-to-noise ratio of the raw data was adequate.

Since the materials are highly air sensitive, precautions and care must be taken in order to measure the components in an oxygen-free environment. The samples previously sealed under He gas atmosphere in a capillary were mounted on the sample holder of the different spectrometers in a He gas glove box. The sample holders are so designed to allow an oxygen-free transportation of the samples from the He gas glove box within the spectrometers. This allows furthermore a complete removal of the capillary (where the samples were sealed) for the optical investigations. The measurements in various spectrometers were then performed in vacuum or He gas atmosphere conditions, so that the samples were never exposed to air contamination.

Figure 2 shows the optical reflectivity of K_3C_{60} and Rb_3C_{60} in the normal state at 25 and 40 K, respectively. We immediately observe the clear metallic characteristic of the spectra with a well defined plasma-edge behavior at about 5×10^3 cm^{-1}. In Fig. 3 we present the optical reflectivity measured above and below the superconducting transition temperature, in the spectral range which covers the (expected) superconducting gap values. While at low frequencies the reflectivity in the normal state is well described by the so-called Hagen-Rubens extrapolation (see dashed-double-dotted line in Fig. 3), we observe below T_c a clear enhancement of $R(\nu)$ in FIR at frequencies below 100 cm^{-1}, with an onset as a function of temperature coincident with T_c.

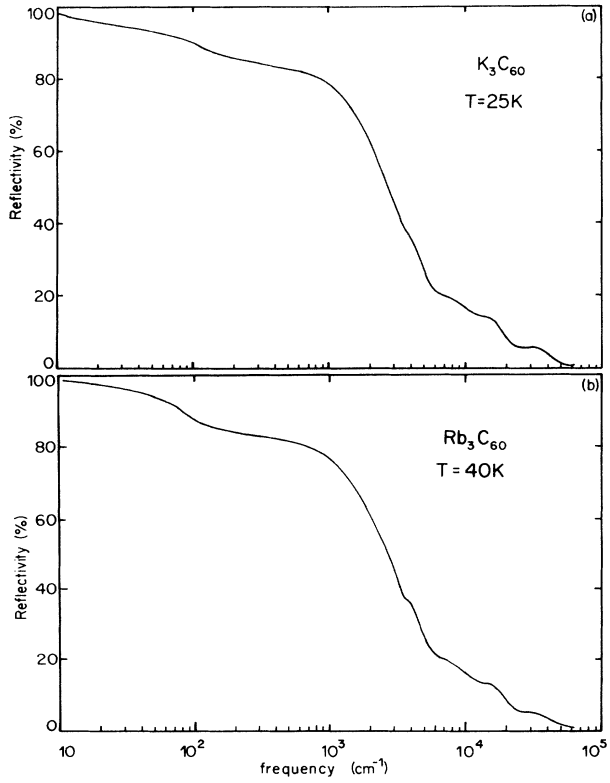

FIG. 2. Reflectivity spectra for (a) K_3C_{60} and (b) Rb_3C_{60} at 25 and 40 K, respectively.

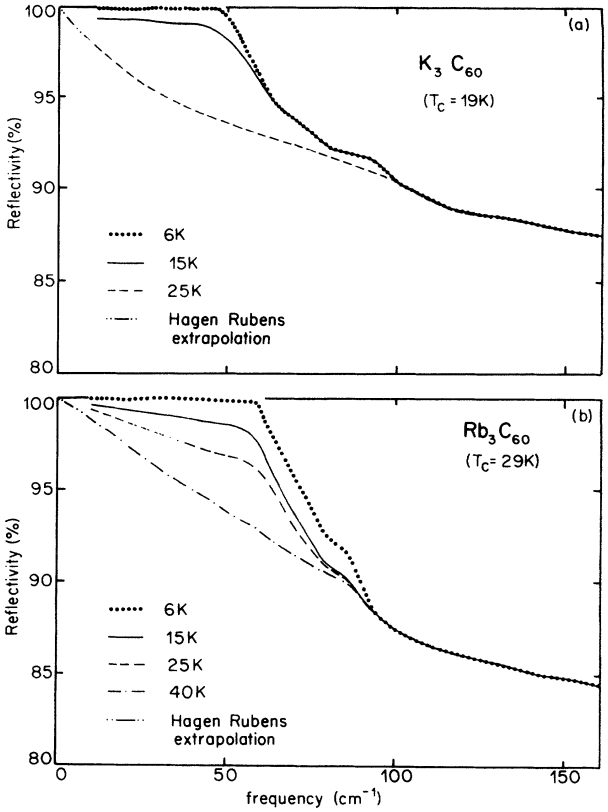

FIG. 3. Optical reflectivity at several temperatures in the infrared spectral range for (a) K_3C_{60} and (b) Rb_3C_{60}.

The optical conductivity is then obtained through Kramers-Kronig (KK) transformation of $R(\nu)$. For this purpose the $R(\nu)$ spectra above T_c have been extrapolated to zero frequency by means of the Hagen-Rubens relation using the measured σ_{dc} values[12] and beyond the highest measurable frequency (5×10^4 cm^{-1}) by the well known $R(\nu)\sim1/\nu^2$ and $R(\nu)\sim1/\nu^4$ (for $\nu>1\times10^5$ cm^{-1}) extrapolations. Our reflectivity spectra at 6 K are equal to 100%, within the experimental error of 0.5%, up to a well defined threshold frequency of 48 cm^{-1} for K_3C_{60} and 60 cm^{-1} for Rb_3C_{60} (see Fig. 3). The experimental error of 0.5% in the reflectivity measurements gives an error range of ±100 $(\Omega\,\text{cm})^{-1}$ for the optical conductivity σ_1 obtained from the KK transformation. In order to avoid unphysical scattering in the absolute values of σ_1 at 6 K we have used the extrapolation $R(\nu)=100\%$ between $\nu=0$ and the threshold frequencies of 48 and 60 cm^{-1} for K_3C_{60} and Rb_3C_{60}, respectively. The complete excitation spectrum in the normal state is presented in Figs. 4 and 5. In Fig. 5 we compare our KK results for K_3C_{60} with the optical conductivity evaluated from the reflectivity spectrum of Iwasa *et al.* (see inset).[15] Figure 6 displays $\sigma_1(\nu)$ in FIR at temperatures corresponding to the normal state and well below T_c (i.e., 6 K).

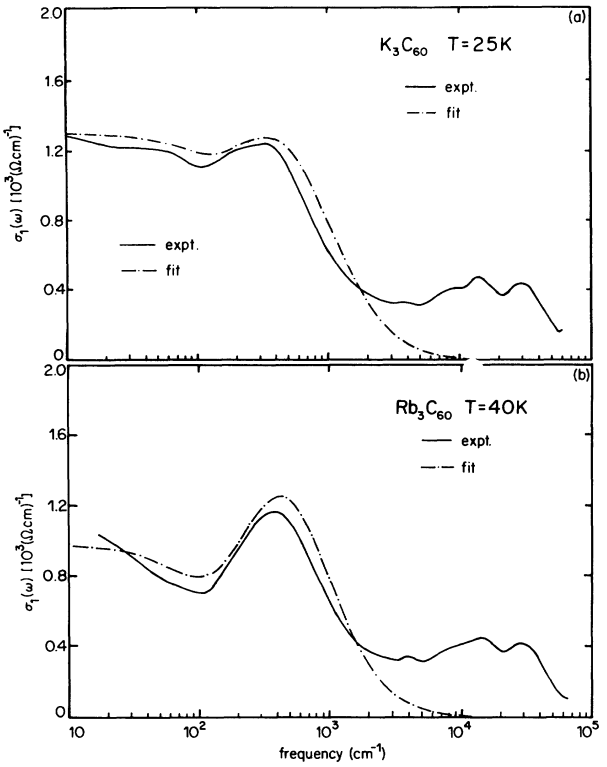

FIG. 4. Normal-state optical conductivity for (a) K_3C_{60} and (b) Rb_3C_{60} at 25 and 40 K, respectively, as evaluated, from KK analysis. The phenomenological fit (dashed-dotted line), based on Eq. (2), is discussed in the text, and the parameters are summarized in Table I.

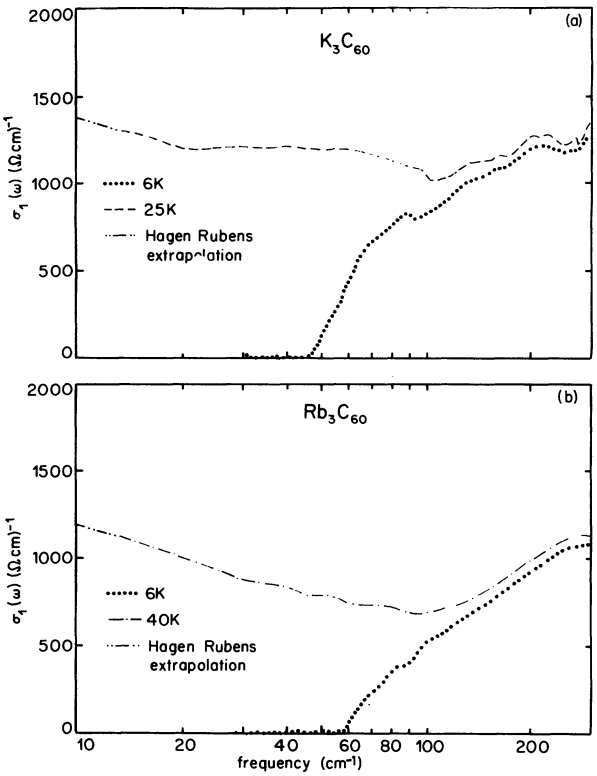

FIG. 6. The optical conductivity above and below T_c for (a) K_3C_{60} and (b) Rb_3C_{60}, evaluated from the reflectivity data of Figs. 2 and 3 (note the logarithmic frequency scale).

III. DISCUSSION

A. Normal state

We first note, that $\sigma_1(\nu)$, as shown in Fig. 4, is remarkably different from that of a simple metal, where the Drude model is appropriate and for which the so-called total spectral weight is given by the expression

$$\int_0^\infty \sigma_1(\omega)d\omega = \frac{\pi n e^2}{2m_b} = \frac{\omega_p^2}{8} \tag{1}$$

with n the number of carriers and m_b the band mass. Instead, we observe a Drude-like response—which, however, does not lead to the oscillator strength as given by Eq. (1)—together with a mid-infrared absorption. At higher

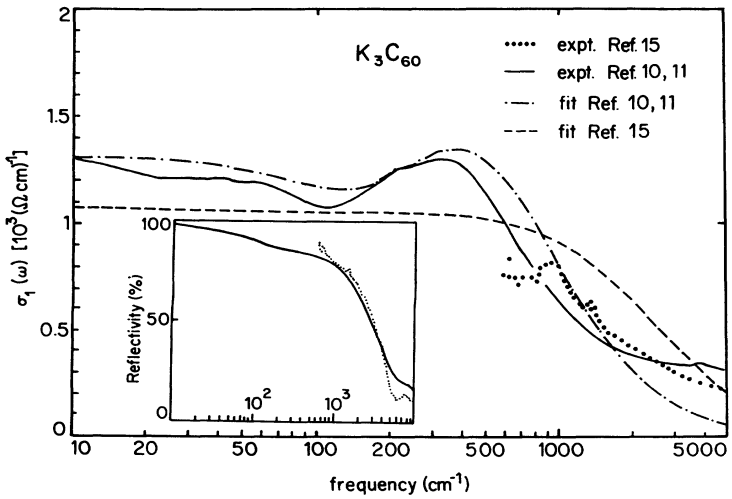

FIG. 5. Optical conductivity of K_3C_{60} evaluated from KK transformation of the $R(\nu)$ spectra of Fig. 2 and of Ref. 15, together with the phenomenological fits (see text). The inset displays our reflectivity spectrum and of Ref. 15 below the plasma edge.

frequencies ($\nu > 2000$ cm^{-1}), we also observe several absorptions due most probably to interband transitions. It is worth noting that the overall behavior of $\sigma_1(\nu)$ is similar to that observed in various correlated materials with low electron density, notable the high-T_c oxides,[16] $BaBi_xPb_{1-x}O_3$,[17] and certain organic conductors.[18] Several mechanisms, based on electron-electron or electron-phonon interactions, were suggested in order to explain the particular or nonconventional behavior of $\sigma_1(\nu)$ (for a review see Ref. 16) in these materials.

Next, we discuss the essential features of our experimental result and compare our findings with band-structure calculations and other experimental parameters. At high frequencies (i.e., from the visible to the UV) our excitation spectrum is characterized by broad transitions peaked at approximately 4×10^3 cm^{-1}, 1.8×10^4 cm^{-1} (with a shoulder at approximately 1×10^4 cm^{-1}), and 3.5×10^4 cm^{-1}. We ascribe these excitations to the interband transitions involving s and p carbon orbitals and s, p, and d alkali orbitals. Our measured conductivity or correspondingly the imaginary part of the dielectric function [$\sigma_1(\nu)=0.5\nu\varepsilon_2(\nu)$] is in good accord with the theoretical predictions extracted from a band-structure calculation,[19] which leads to broad peaks centered at approximately 1 eV (8.07×10^3 cm^{-1}), 2.5 eV (2.02×10^4 cm^{-1}), and 4 eV (3.23×10^4 cm^{-1}) [see Fig. 3(b) of Ref. 19]. This calculation[19] also predicts weak optical electronic transitions (seen by energy-loss spectroscopy[20]) above 4.5 eV ($\sim4\times10^4$ cm^{-1}), which however we do not observe, presumably due to the very low reflectivity in this frequency range.

The low-frequency part of $\sigma_1(\nu)$ (i.e., from FIR up to mid-IR) is characterized by two main features: the broad band centered at approximately 500–800 cm^{-1} and the Drude-like contribution to $\sigma_1(\nu)$ at FIR frequencies. In view of these features we model the dielectric function with the following expression:

$$\varepsilon(\nu)=\varepsilon_\infty+\nu_p^2\left[\frac{f_G}{\nu_G^2-\nu^2-i\nu\gamma_G}-\frac{1-f_G}{\nu(\nu+i\gamma_D)}\right], \qquad (2)$$

where ε_∞ describes the high-frequency contribution to the dielectric function, while the second and third term in the brackets describe the mid-IR broad excitation and the Drude-like response at low frequencies, respectively. The best fit, shown in Fig. 4 by the dashed-dotted line, is obtained with the parameters summarized in Table I. We note, that a frequency-dependent relaxation rate would improve the agreement between $\sigma_1(\nu)$ and the Drude part of the fit in the FIR. This would, however, introduce new parameters, the discussion of which will be far beyond the phenomenological nature of our approach.

Starting with formula (2) there are two main directions that can be followed to interpret our spectroscopic data. The first one, which we will call the one-component picture, is based on the assumption that the low-frequency Drude-like behavior and the harmonic oscillator for the mid-IR absorption are due to the response of the conduction band, and crudely speaking the charge carriers (which from simple chemical counting arguments should be $n=4.1\times10^{21}$ cm^{-3}) behave as free carriers at low frequencies and as bound ones at high frequencies. This interpretation is similar to that often applied to the high-T_c Cu-O superconductors and also some heavy fermion materials, where also a simple Drude model cannot describe $\sigma_1(\nu)$.[16] Frequency-dependent mass renormalization due to electron-electron interactions, and alternatively midgap states (like polarons or excitons) or a broad phonon spectrum (i.e., the Holstein process) were suggested as a source of the frequency-dependent scattering at FIR and mid-IR frequencies. The total spectral weight, corresponding to the plasma frequency $\nu_p=9491$ cm^{-1} for K_3C_{60} and 9220 cm^{-1} for Rb_3C_{60}, would imply an effective band mass $m_b\sim4m_e$ with $n=4.1\times10^{21}$ cm^{-3}. This value is somewhat smaller than the value arrived at from spin susceptibility measurements, $m_b=6.5m_e$.[21] From the plasma frequency we calculate a London penetration depth $\lambda_L=c/(2\pi\nu_p)=1677$–$1726$ Å (appropriate in the clean limit), somewhat smaller than the measured value (see below) and in broad agreement with the theoretical value of 1600 Å of Erwin and Pickett.[22]

The second way to interpret Eq. (2) is to consider the two contributions independently, using a two-component picture. Then, the Drude part is characterized by a plasma frequency of $\nu_p^*=3307$ cm^{-1} for K_3C_{60} and 2420 cm^{-1} for Rb_3C_{60} [i.e., $\nu_p^*=(1-f_G)^{1/2}\nu_p$], and the harmonic oscillator is viewed as a separate mid-IR excitation. We first note that the scattering rate (γ_D) of the Drude component is in good agreement with the evaluation of Klein *et al.*[12] from $\rho(T)$ measurement and is larger than the superconducting gap 2Δ as evaluated from tunneling spectroscopy measurements (100 cm^{-1} for Rb_3C_{60}) (Ref. 7) and from nuclear-magnetic-resonance experiments (29.5 cm^{-1} and 65 cm^{-1} for K_3C_{60} and Rb_3C_{60}, respectively).[23] This suggests that the K_3C_{60} and Rb_3C_{60} compounds are in the dirty or nearly dirty limit. Of course, the relaxation rate may also be dominated by intergrain scattering. Thus, because of the granularity, our measured $1/\gamma_D$ is a lower limit for the relaxation scattering time, and in single crystals a larger

TABLE I. Parameters for the phenomenological fit using Eq. (2): the total plasma frequency ν_p, and the damping γ_D for the Drude term, the resonance frequency ν_G and the damping γ_G for the harmonic oscillator, and finally the high-frequency contribution to the dielectric function ε_∞. f_G represents the weight factor between the Drude term and the harmonic oscillator.

	ν_p cm^{-1}	γ_D cm^{-1}	ν_G cm^{-1}	γ_G cm^{-1}	ε_∞	f_G
K_3C_{60}	9491	147	444	1210	5	0.878
Rb_3C_{60}	9220	100	444	1089	6	0.931

$\tau_D \sim 1/\gamma_D$ is expected. However, there are some severe problems with this two-component picture. In fact, the small plasma frequency associated with the Drude response of the free charge carriers would imply a large effective band mass (i.e., $m^* \sim 30m_e$ and $m^* \sim 63m_e$ for K-and Rb-doped C_{60}, respectively) unless a smaller effective number of carriers ($n_{\text{eff}} < n = 4.1 \times 10^{21}$ cm^{-3}) is considered. This strong renormalization of the normal-state optical properties (within the two-component phenomenological approach) might be suggestive of the important role played by correlation effects (see below).

In view of the rather peculiar behavior of $\sigma_1(\nu)$ Fig. 5 is particularly pertinent. We compare indeed our optical conductivity of K_3C_{60} with that calculated from the KK transformation of the $R(\nu)$ spectrum measured by Iwasa *et al.*[15] The corresponding reflectivity curves are displayed in the inset of Fig. 5. The overall agreement between the two sets of data (particularly below 5×10^3 cm^{-1}) indicates that our pressed pellet specimens are of good quality, thus suggesting that particle size effects or granularity should not play an important role. However, while in general the electrodynamic response is similar in the frequency range common to both set of data, important differences appear in the far infrared (FIR). In fact, a careful inspection of our $R(\nu)$ shows that below approximately 500 cm^{-1} (i.e., the lowest frequency limit of Ref. 15) there is an inflexion point in the spectra. The low-frequency behavior, entirely missed by Iwasa *et al.*, has a considerable influence for the Kramers-Kronig (KK) transformation, as discussed above. In order to enhance this aspect, we also present our phenomenological fit (i.e., Drude term and mid-IR harmonic oscillator) and the simple Drude term calculated with the parameters of Ref. 15 (i.e., $\nu_p = 1.26 \times 10^4$ cm^{-1} and $\gamma_D = 2484$ cm^{-1}). It is clear from the figure that a simple Drude can fit appreciably well $\sigma_1(\nu)$ on the high-frequency side but it is not appropriate down to FIR. Therefore, this comparison further points out the importance of low-frequency measurements (i.e., down to FIR) for a complete understanding of the excitation spectrum and in order to avoid misleading conclusions. Nevertheless, it is interesting to remark that the plasma frequency ($\nu_p = 1.26 \times 10^4$ cm^{-1}), used in the simple Drude approach by Iwasa *et al.*,[15] is in fair agreement with our evaluation from the total spectral weight (i.e., $\nu_p = 9220$–9491 cm^{-1}).

As far as the broad mid-IR excitation within this two-component picture is concerned, we were very tempted, in our first optical investigations,[10] by a photoemission and bremstrahlung result, which indicates a pseudogap-like structure at about 4×10^3 cm^{-1}.[24] We found this possibility for the interpretation of the mid-IR excitation to be particularly compelling in view of the similarity between the optical spectra of the alkali-doped C_{60} and of $BaBi_xPb_{1-x}O_3$ [with $x = 0.3$ and superconducting transition at $T_c = 12$ K (Refs. 17 and 25)]. In fact, the occurrence of a pseudogap in the density of states of this correlated material was envisaged and a similar phenomenological description based on Eq. (2) was considered for the corresponding optical conductivity.[17] Nevertheless, besides the fact that our absorption appears at a frequency much lower than 0.5 eV, recent photoemission results[26] question the pseudogap intepretation given by Takahashi *et al.*[24] It appears that the spectra reported in Ref. 26 do not show any signs of a pseudogap at the Fermi level and it is suggested that the discrepancy between these two sets of data lies most probably in the *different* composition of the samples studied by photoemission.[24,26] It is believed that the spectra given in Ref. 24 represent the situation of a much higher K-doping level (i.e., $x > 3$). Therefore, we now consider the pseudogap possibility quite unlikely for the explanation of the mid-IR excitation. However, we suggest that it can be assigned to an electronic transition. Indeed, band-structure calculations also hint at the presence of absorptions below 0.1 eV (800 cm^{-1}).[19]

Alternatively, we must also consider a phononic origin for this mid-IR absorption. It is well established that strong phonon activity is expected in this mid-IR frequency range. Besides the bare IR-active phonon modes, it has been suggested that in A_xC_{60} a so-called dopant-induced charge-phonon effect (i.e., T_{1u} modes acquire charge via coupling to virtual $t_{1u} - t_{1g}$ transitions) and coupling of Raman-active phonon modes (with H_g and A_g symmetry) with electron $t_{1u} - t_{1u}^*$ interband transition may occur.[27,28] Pichler, Matus, and Kuzmany, made a detailed *in situ* IR-transmittance and reflectivity measurements of K-doped C_{60} and found for K_3C_{60} the IR-active T_{1u} modes (enhanced by the charge-phonon mechanism) and some additional weak structures, overlapped to the broad mid-IR absorption.[29] They assigned those features to Fano-distorted Raman-active H_g and A_g modes. Similar results have been also obtained by Martin, Koller, and Mihaly with *in situ* infrared transmission.[30] As already mentioned, in our $\sigma_1(\nu)$ we just have evidence of the broad feature at about 500–800 cm^{-1}, but we do not find the IR-active T_{1u} modes and the Fano-distorted Raman modes. We should, however, remark that for A_3C_{60} (i.e., the metallic compound) both phononic features were found to be fairly weak in the transmission measurements and even more so in the reflectivity ones.[29,30] Moreover, Iwasa *et al.* did not find the Fano-distorted Raman resonances but only the T_{1u} modes.[15] Furthermore, since the mode strength of the IR-active T_{1u} modes scales with x^2 (x being the alkali-doping),[27] it also turns out that the features seen by Pichler, Matus, and Kuzmany[29] would be more consistent with the $x = 4$ doping. Thus, it might well be that, besides a reduced resolution in our measurement due to the surface scattering of our pressed pellets, for $x = 3$ compound the free-electron plasma-edge behavior screens these excitations. Even though this phononic activity, although screened or smeared by the free electrons, might be another important source of absorptions, it remains to be seen and it is still matter of debate whether a purely electronic transition or a phononic activity (or a combination of both) is the main cause for this mid-IR absorption.

An exact determination of the origin of this mid-IR excitation would also be of fundamental importance, in order to single out which one of the two pictures (i.e., the

one- or two-component approach) applies. Unfortunately, the calculation of the mean free path $l=v_F\tau_D$, as well, cannot help in solving this puzzling aspect. In fact, the strong renormalization of the normal-state properties, represented phenomenologically by the enhancement of the effective mass within the two-component picture, cancels out in the evaluation of l (i.e., v_F will be reduced by m^* but also τ_D is enhanced by m^*). Furthermore, the evaluation of l is only tentative, since it depends rather strongly on several assumptions and one finds values ranging in a fairly broad interval. However, assuming the one-band free-electron model with charge-carrier concentration $n=4.1\times10^{21}$ cm^{-3}, we obtain $l=5-10$ Å within the two-component picture. For comparison we quote the value $l=3.6$ Å reported by Iwasa *et al.*, within a simple Drude term approach.[15] We remark that l is smaller than the lattice constant of about 14 Å. Moreover, regardless of the way l has been obtained, its value is also smaller than or comparable to the coherence length as evaluated from the measurement of the upper critical field H_{c2}, i.e., $\xi\sim30$ Å.[31] Once again, this places our compounds in the dirty limit, and confirms our previous inferences about the relaxation scattering rate.

Nevertheless, the nonsimple Drude behavior of the low-frequency optical conductivity remains the main point of discussion and among theorists it is a matter of debate. Here, we point out that several theoretical models, based on the effect of the structural disorder, reproduce, sometimes only qualitatively, the experimental behavior of $\sigma_1(\nu)$ in the normal state. We mention for instance the work of Gelfand and Lu, who calculated, starting from a tight-binding method, the dc and ac transport properties (i.e., the optical conductivity) for different degrees of orientational disorder of the C_{60} molecules.[32–34] By increasing the orientational disorder (which appears to persist even at low temperatures) an absorption band, overlapped to a low-frequency Drude term, develops progressively in a way similar to our experimental findings.[33,34] Liechtenstein *et al.* also studied the effect of structural disorder and they found that A_3C_{60} is not three-dimensionally disordered but ordered in two dimension and disordered in the third.[35] Their calculated optical conductivity is once again far from being a simple Lorentzian. It is indeed the sum of a Drude-like contribution and an interband Lorentzian peak at about 500 cm^{-1}.[35] Of course, these models imply a fully electronic origin of the mid-IR absorption (they do not take into account any kind of electron-phonon coupling). Whether these models can completely describe the experimental data (also in relation to the mechanism for the superconductivity) remains to be seen but they are a further indication of the rather complex behavior of the optical conductivity in the normal state.

B. Superconducting state

The discussion of the superconducting-state optical properties is somehow more straightforward than for the normal one. Figure 6 displays the optical conductivity in the normal state (see also Fig. 4) and at 6 K (which is low enough, relative to T_c, to be considered as the experimental limit of the $T=0$ superconducting ground state) in the frequency range relevant for the expected superconducting gap. It is clearly shown that for both compounds the conductivity is zero up to a threshold frequency which we identify as the superconducting gap. We obtain $\Delta=24$ cm^{-1} for the K and 30 cm^{-1} for the Rb compound. Together with the superconducting transition temperatures $T_c=19$ and 29 K this leads to the ratio $2\Delta/k_BT_c=3.6$ and 2.98 for K_3C_{60} and Rb_3C_{60}, with both values in good agreement with the weak-coupling BCS result of $2\Delta/k_BT_c=3.52$. This would suggest that the relevant excitation, responsible for superconductivity pairing, is significantly larger than the energy associated with the single-particle gap in these materials.

Recently, several experimental results obtained with various techniques were also found to be in very good agreement with the weak-coupling limit of the BCS theory. Particularly, we quote the specific-heat, isotope effect, and normal-state susceptibility investigations by Ramirez and co-workers,[36,37] the pressure and temperature dependence of the nuclear-spin-lattice relaxation of Quirion *et al.*[38] and finally the muon-spin-relaxation (μSR) experiments by Kiefl *et al.*[39] The analysis of the specific-heat jump ΔC at T_c and of the normal-state susceptibility of A_3C_{60} (Ref. 37) together with the isotope shift data (Ref. 36) within a phonon-mediated interaction framework provides a consistent picture of superconductivity as arising from exchange of high-energy (>1000 K) intramolecular phonons. Furthermore, the small ΔC along with the known upper critical field slope gives evidence for a dirty limit superconductor, with mean free path $l\sim10$ Å,[37] in agreement with our estimate. Also Quirion *et al.* found that, within a BCS approach for the expression of T_c, the reduction of the electronic density under pressure is found to favor a pairing mechanism involving high-frequency intramolecular vibrations.[38] In addition to that, the temperature dependence of the muon T_1^{-1} spin relaxation shows a coherence peak just below T_c, which can be fit to the conventional Hebel-Slichter theory with a broadened BCS density of states.[39] Moreover, the average energy gap is consistent with the BCS weak-coupling limit.[39] On the other hand and as already anticipated in the introduction, a tunneling measurement leads to a contrasting result, claiming a gap ratio $2\Delta/k_BT_c\sim5$, which would place these systems well into the strong-coupling limit of the BCS approach.[7] Although a full understanding of this controversy has not been yet reached, we will return to this issue later in the discussion.

A further step in the analysis of our optical conductivity data can be performed by applying so-called spectral weight arguments. In fact, using the electrodynamic sum rule, one can evaluate the penetration depth in the superconducting state. From the missing spectral weight, the penetration depth is given by[40]

$$\lambda^2=\frac{c^2}{8A},\quad A=\int_0^{\infty}[\sigma_{1,n}(\nu)-\sigma_{1,s}(\nu)]d\nu\,, \tag{3}$$

where c is the speed of light, and $\sigma_{1,n}$ and $\sigma_{1,s}$ are the optical conductivity in the normal and superconducting

state, respectively. We performed the integral A up to the frequency where $\sigma_{1,n}$ and $\sigma_{1,s}$ are no longer different within the experimental error of our measurement,[41] and we obtain $\lambda = 8000 \pm 500$ Å for the two compounds, in satisfactory agreement with the penetration depth of 6000 Å (Ref. 23) or 4800 Å (Ref. 42) for K_3C_{60}, and 3700 Å (Ref. 39), 4600 Å (Ref. 23) or 4200 Å (Ref. 43) for Rb_3C_{60}. These values are, however, larger than the London penetration depth evaluated by Erwin and Pickett.[22]

Even though we will discuss our optical results in terms of a sophisticated approach, based on the Eliashberg theory of the superconductivity (see Sec. III C), it is nevertheless instructive to perform a first comparison with the more conventional electrodynamic response calculation of Mattis and Bardeen within the framework of the BCS theory.[44] The functional form of $\sigma(\nu)$ in the superconducting state corresponds to the expressions[44]

$$\frac{\sigma_{1s}}{\sigma_{1n}} = \frac{2}{\hbar\omega}\int_{\Delta}^{\infty}[f(E)-f(E+\hbar\omega)]g(E)dE + \frac{1}{\hbar\omega}\int_{\Delta-\hbar\omega}^{-\Delta}[1-2f(E+\hbar\omega)]g(E)dE \ , \tag{4}$$

$$\frac{\sigma_{2s}}{\sigma_{1n}} = \frac{1}{\hbar\omega}\int_{\alpha}^{\Delta}\frac{[1-2f(E+\hbar\omega)](E^2+\Delta^2+\hbar\omega E)dE}{(\Delta^2-E^2)^{1/2}[(E+\hbar\omega)^2-\Delta^2]^{1/2}} \ , \tag{5}$$

where

$$\alpha = \Delta - \hbar\omega \ \text{ for } \hbar\omega < 2\Delta \text{ or } \alpha = -\Delta \ \text{ for } \hbar\omega > 2\Delta \ ,$$

$$f(E) = \frac{1}{e^{E/k_BT}+1} \ ,$$

$$g(E) = \frac{(E^2+\Delta^2+\hbar\omega E)}{(E^2-\Delta^2)^{1/2}[(E+\hbar\omega)^2-\Delta^2]^{1/2}} \ ,$$

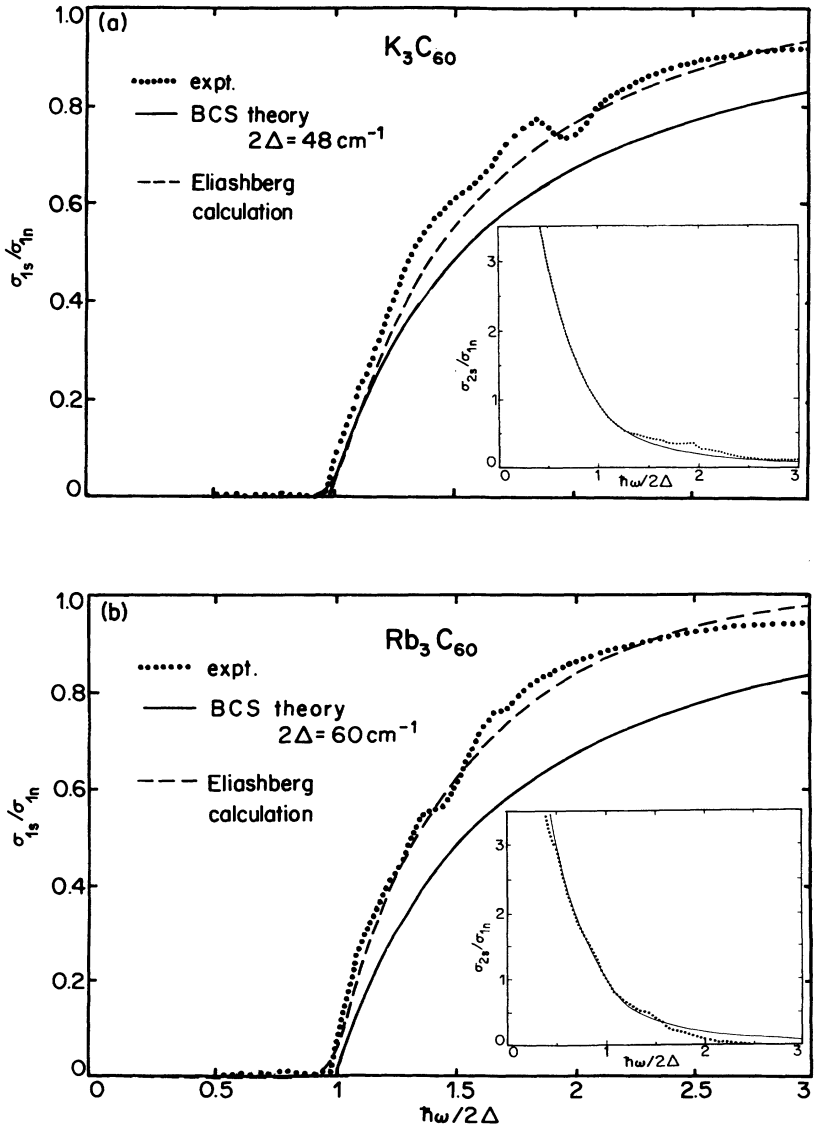

FIG. 7. The measured optical conductivity together with $\sigma_{1,s}(\nu)/\sigma_{1,n}(\nu)$ calculated using the Mattis-Bardeen theory (BCS) with the single-particle gap values given in the text. The insets show the imaginary part $\sigma_{2,s}(\nu)/\sigma_{1,n}(\nu)$. The dashed curve corresponds to the fit within the Eliashberg approach (see text, Sec. III C) with an impurity parameter of $1/\tau = 200\ cm^{-1}$ and $194\ cm^{-1}$ for K_3C_{60} and Rb_3C_{60}, respectively.

which in the $T \rightarrow 0$ limit reduce to the formulas

$$\frac{\sigma_{1s}}{\sigma_{1n}} = \left[1+\frac{2\Delta}{\hbar\omega}\right]E(k)-\frac{4\Delta}{\hbar\omega}K(k), \quad \hbar\omega > 2\Delta \qquad (6)$$

$$\frac{\sigma_{2s}}{\sigma_{1n}} = \frac{1}{2}\left[1+\frac{2\Delta}{\hbar\omega}\right]E(k')-\frac{1}{2}\left[1-\frac{2\Delta}{\hbar\omega}\right]K(k') , \qquad (7)$$

where $k=(\hbar\omega-2\Delta)/(\hbar\omega+2\Delta)$, $k'=(1-k^2)^{1/2}$, and $E(k)$ and $K(k)$ are the tabulated complete elliptic integrals. The latter expressions are dependent only on the gap frequency. Equations (6) and (7), together with the measured optical conductivity, are displayed for both compounds in Fig. 7. [We note that the thermal broadening corrections introduced by the finite temperature of 6 K through Eqs. (4) and (5) are here very negligible.] Given the fact, that the calculation neglects the role played by mean-free-path effects, the agreement between our results and the theory based on a BCS ground state is excellent. Particularly outstanding is the agreement for $\sigma_{2,s}$ (see insets), where the $1/\nu$ behavior is recovered at low frequencies. We also note, that the functional form reflects the so-called case II coherence factors,[40] which depend sensitively on the symmetry of the superconducting wave function, and therefore the agreement between theory and experiment gives clear evidence for a singlet ground state.

Until now we have discussed two limiting cases; namely the normal-state and the superconducting ground-state limit (i.e., 6 K). However, Fig. 3 displays also the reflectivity spectra for several temperatures below T_c. An alternative representation, which would further enhance that temperature dependence, corresponds to the so-called relative reflectivity R_s/R_n. This is shown in Fig. 8 for both compounds. Our results are in good agreement with previous ones[8] and at the lowest temperature (i.e., 6 K) they agree fairly well with the calculation of R_s/R_n within the BCS weak-coupling limit (N.B. we have assumed a simple Drude with $\nu_p=9680$ cm^{-1} and $\gamma_D=1210$ cm^{-1} for the normal-state dielectric function). Nevertheless, the temperature dependence of the optical spectra by increasing the temperature towards T_c is rather anomalous. The peak of R_s/R_n (which actually defines the frequency of the superconducting gap 2Δ) does not shift to lower energies as predicted by the Mattis-Bardeen calculation within the BCS theory. Previous experiments in reflectivity[8] and transmission[9] are also plagued by the same problems. There are several possible explanations for this anomalous temperature dependence of the superconducting gap. First of all, it might reflect a distribution of gaps due to materials with different T_c (i.e., an inhomogeneity of the specimens) or to a gap anisotropy on the Fermi surface. Indeed, Fitzgerald *et al.* were able to reproduce their T_s/T_n measurements within an effective-medium approximation consisting of materials with different gaps.[9] Of course, the thermal screening might also play an important role and cannot be excluded *a priori*. As consequence of that, the intrinsic temperature dependence would be beyond the experimental resolution.

We have already pointed out very briefly that there is

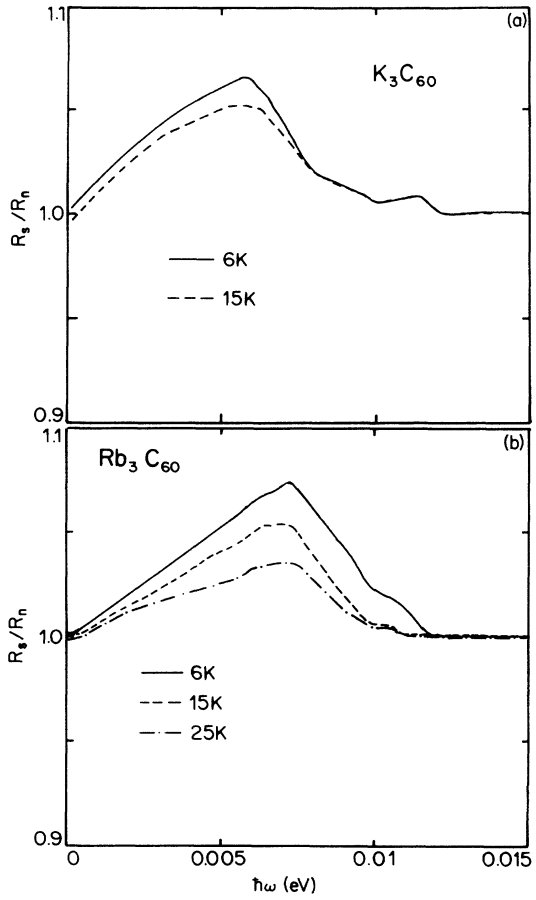

FIG. 8. Reflectivity ratio $R_s(T<T_c)/R_n(T_n)$ for (a) K_3C_{60} and (b) Rb_3C_{60} (with $T_n=25$ and 40 K, respectively).

an apparent disagreement between the optical results,[8,9,11] suggesting the BCS weak-coupling limit, and the tunneling[7] experiments, consistent with the strong-coupling one. One should remark that tunneling experiments, because of the extreme air sensitivity of these materials, may be subject to surface effects with Δ different in the surface layers than in the bulk. Nevertheless, a recent calculation of the zero-temperature density of states $\rho_s(\varepsilon)$, using the *multi*band superconductivity gap equation, might be of help in order to reconcile these contradictory results.[45] It is shown that $\rho_s(\varepsilon)$ displays a broad shoulder with onset at $2\Delta/k_BT_c \sim 3$ and a sharp peak at $2\Delta/k_BT_c \sim 5$. Thus, the tunneling measurement [which *directly* measures $\rho_s(\varepsilon)$] may be sensitive to the peaks in $\rho_s(\varepsilon)$, while optical investigations (which, however, measure the joint density of states) may detect the lowest possible excitation across the superconducting gap. It should also be noted that a careful inspection of the tunneling results reveals a fairly large broadening of the gap feature, which deviates from the ideal BCS expression.[7] In Ref. 7 it is suggested that this broadening could be caused by inelastic scattering or strong-coupling effects. Moreover, the recent μSR experiment shows a reduced Hebel-Slichter peak, compared to the BCS prediction within a single-band model.[39] This result might be another indication for a significant broadening in the den-

sity of states. Therefore, based on this recent calculation,[45] the discrepancy of the gap ratio determined from tunneling and optical measurements could be traced to the difference of the definition of the "gap."

C. The predictions of conventional theory

It is of interest to compare now the experimental results with the predictions of the conventional electron-phonon theory of superconductivity, in a more complete fashion, however, than the BCS approach. To this end we describe our use of the standard Eliashberg theory to calculate the optical conductivity for arbitrary impurity scattering in the local approximation. Eliashberg theory describes all properties of the conventional superconductors to within a few percent and is considered to be one of the most exact theories in condensed-matter physics.[46] While it reduces to the standard weak-coupling BCS theory in the limit of the average phonon frequency being much greater than T_c and the renormalization parameter $\lambda=0$, the full theory takes into account the full details of the retarded electron-phonon interaction. With regard to the optical properties, the formalism has in the past,[47–50] and also more recently[51] been used to calculate the conductivity of conventional superconductors such as Pb and Nb and good agreement with experiment has been achieved beyond the Mattis-Bardeen theory[44] with regard to Holstein structure and impurity scattering. Note that the conventional Mattis-Bardeen theory of optical conductivity corresponds to a weak-coupling superconductor with no phonon structure and in the dirty limit ($1/\tau\rightarrow\infty$). Development of formalism for the calculation of optical conductivity for arbitrary impurity scattering in the superconducting state has only recently been put forward.[52,53] This recent work includes both impurity- and phonon-assisted absorption processes whereby a photon creates a hole-particle pair in the metal and this pair relaxes through impurity or phonon scattering (this latter process being termed the Holstein process).

The complex optical conductivity is calculated from the current-current correlation function and given in the local limit ($\mathbf{q}\rightarrow 0$) as[53]

$$\sigma(\omega,T)=\frac{i}{\omega}\Pi(i\nu_m\rightarrow\omega+i0^+)\ , \tag{8}$$

where the current-current correlation function is given as[53]

$$\Pi(i\nu_m)=\frac{T}{N}\sum_{n\mathbf{k}}\mathrm{Tr}\frac{ek_x}{m}G[\mathbf{k},i(\omega_n+\nu_m)]G(\mathbf{k},i\omega_n)\Gamma_x\ . \tag{9}$$

In this formula we neglect vertex corrections by making the approximation $\Gamma_x=ek_x/m$. This is a standard approximation in conventional superconductors where this is equivalent to the use of the usual $\alpha^2F(\omega)$ and quasiparticle scattering time τ^{qp} instead of using the corresponding transport quantities, $\alpha^2_{\mathrm{tr}}F(\omega)$ and $\tau^{\mathrm{qp}}_{\mathrm{tr}}$.[54] In general for an s-wave superconductor with no unusual momentum dependence in the electron-phonon interaction, neglect of vertex corrections is acceptable. We will assume that this is also the case for the doped fullerenes.

Following Bickers *et al.*,[53] $\Pi(i\nu_m)$ is given in terms of the plasma frequency ω_p, the Matsubara gaps $\tilde{\Delta}_n$, and renormalization factors $\tilde{\omega}_n$ by

$$\Pi(i\nu_m)=\frac{\omega_p^2}{4\pi}\pi T\sum_n S_{nm} \tag{10}$$

with

$$\begin{aligned}S_{nm}&=\frac{\tilde{\omega}_n(\tilde{\omega}_n+\tilde{\omega}_{n+m})+\tilde{\Delta}_n(\tilde{\Delta}_n-\tilde{\Delta}_{n+m})}{R_nP_{nm}}-\frac{\tilde{\omega}_{n+m}(\tilde{\omega}_{n+m}+\tilde{\omega}_n)+\tilde{\Delta}_{n+m}(\tilde{\Delta}_{n+m}-\tilde{\Delta}_n)}{R_{n+m}P_{nm}}\ ,\quad \text{for } m\neq 0,-2n-1\\&=\frac{\tilde{\Delta}_n^2}{R_n^3},\quad m=0\\&=\frac{1}{R_n},\quad \text{for } m=-2n-1\ .\end{aligned} \tag{11}$$

In Eq. (11), $R_n=\sqrt{\tilde{\omega}_n^2+\tilde{\Delta}_n^2}$ and $P_{n,m}=\tilde{\omega}_n^2-\tilde{\omega}_{n+m}^2+\tilde{\Delta}_n^2-\tilde{\Delta}_{n+m}^2$. The Matsubara renormalized gaps $\tilde{\Delta}_n$ and frequencies $\tilde{\omega}_n$ come from the standard solution of the Eliashberg equations on the imaginary axis[55,56]

$$\tilde{\Delta}_n=\pi T\sum_m[\lambda(m-n)-\mu^*\Theta(\omega_c-|\omega_m|)]\frac{\tilde{\Delta}_m}{\sqrt{\tilde{\omega}_m^2+\tilde{\Delta}_m^2}}+\frac{1}{2\tau}\frac{\tilde{\Delta}_n}{\sqrt{\tilde{\omega}_n^2+\tilde{\Delta}_n^2}} \tag{12}$$

and

$$\tilde{\omega}_n=\omega_n+\pi T\sum_m\lambda(m-n)\frac{\tilde{\omega}_m}{\sqrt{\tilde{\omega}_m^2+\tilde{\Delta}_m^2}}+\frac{1}{2\tau}\frac{\tilde{\omega}_n}{\sqrt{\tilde{\omega}_n^2+\tilde{\Delta}_n^2}}\ . \tag{13}$$

Here $\mu^*=0.1$ is the Coulomb pseudopotential, $\Theta(\omega)$ is the Heaviside function, $\omega_n=(2n+1)\pi T$ with $n=0,\pm1,\pm2,\ldots$, $\tilde{\Delta}_n=\Delta_n(i\omega_n)Z(i\omega_n)$, $\tilde{\omega}_n=\omega_nZ(i\omega_n)$, and $\lambda(n-m)$ is given by

$$\lambda(n-m)=\int_0^\infty\frac{2\omega\alpha^2F(\omega)d\omega}{\omega^2+(\omega_n-\omega_m)^2}\ , \tag{14}$$

where $\alpha^2F(\omega)$ is the electron-phonon spectral function. These equations are based on the standard approximations of a constant density of states and the Migdal approximation which neglects vertex corrections. They can easily be generalized to a nonconstant density of states as was done for the A15 compounds.[57] Like the A15's, the doped fullerenes have a nonconstant density of states at the Fermi level. This will be pursued in future work to incorporate a more realistic description of the isotope effect which is sensitive to this feature. The Migdal approximation may be more serious because of the high phonon frequencies we will use here in our calculations relative to the Fermi energy. Usually $\langle\omega\rangle/E_F \ll 1$ for conventional materials. For the doped fullerenes the Fermi energy is about 300 meV and the average phonon frequencies we will be using are about 100 meV and hence $\langle\omega\rangle/E_F \sim \frac{1}{3}$, which may not be sufficient. However, no work has been done to discover the limit at which Migdal's theorem breaks down. While narrow bands exist in the fullerenes, it is expected that the strong orientational disorder of the balls will delocalize the electrons over several bands. These issues are still open to debate, as is the value of μ^* which some believe is much larger in these compounds.[58] For μ^* we will use the standard value and argue that a larger μ^* will imply a larger λ which in turn will pose problems for a conventional explanation of the optical conductivity.

Our primary goal here is to decide: If these materials are conventional electron-phonon superconductors, then what can the optical conductivity tell us about the phonon spectrum? Is the pairing due to intermolecular phonons at low frequencies or intramolecular phonons at high frequencies or both? To this end we first adopt a model $\alpha^2F(\omega)$ spectrum with the form of a single truncated Lorentzian with peak position at ω_0 and width Γ_0 and truncated at Γ_c, i.e.,

$$\alpha^2F(\omega) \propto \frac{1}{(\omega-\omega_0)^2+\Gamma_0^2} - \frac{1}{\Gamma_c^2+\Gamma_0^2}, \quad |\omega-\omega_0| < \Gamma_c$$
$$= 0, \quad |\omega-\omega_0| > \Gamma_c \ . \tag{15}$$

We do not attempt to fit an exact $\alpha^2F(\omega)$ as the variation of parameter space is quite large. Our aim is simply to examine three models. In one we place a peak at high energy typical of intramolecular phonons and calculate the conductivity, in a second we add a peak at very low energy to simulate librational or intermolecular phonons, and in the third we add an extra peak to the spectrum of the first model at slightly lower energy to see if we can describe the temperature dependence of the resistivity along with the optical data.

The $\alpha^2F(\omega)$ spectrum is used in the Eliashberg equations with $\mu^*=0.1$ and ω_c equal to six times the maximum phonon frequency. The equations are iterated for a solution of the Δ_n and ω_n which in turn are used to calculate $\Pi(i\nu_n)$, which is analytically continued by Padé approximants to give the real frequency axis quantity $\sigma(\omega,T)=\sigma_1(\omega,T)+i\sigma_2(\omega,T)$. The impurity parameter $1/\tau$ is used as a fitting parameter. In addition to the frequency-dependent optical conductivity, we will show the related zero-frequency, temperature-dependent quantities of the normal state (resistivity) and the superconducting state (penetration depth or superfluid density). The London penetration depth is easily seen to be related to $\Pi(0)$ and is given as

$$\lambda(T) = \left[\frac{4}{3}\pi N(0)e^2v_F^2T\sum_{n=1}^{\infty}\frac{\Delta_n^2}{Z_n(\omega_n^2+\Delta_n^2)^{3/2}}\right]^{-1/2} \tag{16}$$

and likewise the resistivity is given by Ziman's resistivity formula[54,59]

$$\rho(T) = \frac{4\pi m}{ne^2T}\int_0^{\infty}\frac{\omega\alpha^2F(\omega)d\omega}{\{\exp[\omega/T]-1\}\{1-\exp[-\omega/T]\}} \tag{17}$$

in which we have again approximated the transport spectral density by the thermodynamic one.

Figure 9 shows a typical $\alpha^2F(\omega)$ spectrum which we have used in our calculations, presented in Figs. 7, 10, and 11. In this case we have coupling to high-energy intramolecular phonons which we have simulated by placing a Lorentzian centered at $\omega_0=1210$ cm^{-1} and with the following parameters: $\Gamma_0=160$ cm^{-1} and $\Gamma_c=320$ cm^{-1} for both K_3C_{60} and Rb_3C_{60}. Generally, as expected, shifting this peak in energy does not affect our conclusions in any way so long as the energy is much greater than T_c (i.e., $\langle\omega\rangle > T_c$). The lower peak (omitted in the phonon spectrum of Rb_3C_{60}) is centered at $\omega_0=363$ cm^{-1} with parameters: $\Gamma_0=40$ cm^{-1} and $\Gamma_c=80$ cm^{-1}. This peak was introduced only to provide a fit to the temperature dependence of the resistivity of K_3C_{60} shown in Fig. 10. Omitting this lower-energy peak does not change our conclusions regarding the optical properties. Used as input in the Eliashberg equations and scaling this spectrum to give the correct T_c of 19 and 29 K, we find that $\Delta=23.6$ and 35.9 cm^{-1}, $2\Delta/k_BT_c=3.57$ and 3.56, and $\lambda=0.513$ and 0.514 for K_3C_{60} and Rb_3C_{60}, respectively.

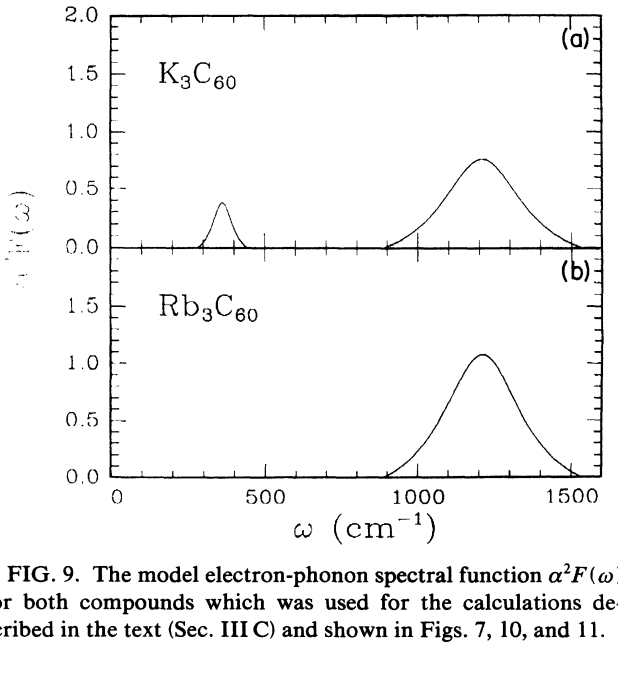

FIG. 9. The model electron-phonon spectral function $\alpha^2F(\omega)$ for both compounds which was used for the calculations described in the text (Sec. III C) and shown in Figs. 7, 10, and 11.

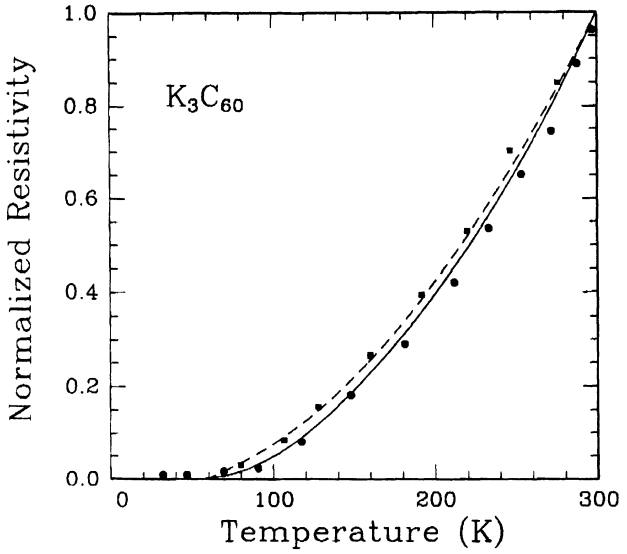

FIG. 10. The temperature-dependent resistivity in the normal state normalized to its value at $T=300$ K, $\rho(T)/\rho(T=300$ K). This normalization was chosen to eliminate the plasma frequency and emphasize the temperature dependence. The dots and squares are the experimental data (see also Fig. 1). The dashed curve is the T^2-empirical fit of the data provided by Klein *et al.*[12] and the solid curve is our calculation using the model $\alpha^2F(\omega)$.

Our solutions for the $\tilde{\Delta}_n$ and $\tilde{\omega}_n$ are now used to calculate the optical conductivity at low temperature and for varying values of $1/\tau$, and we find that an excellent fit to the optical conductivity ratio σ_{1s}/σ_{1n} can be found for $1/\tau \sim 200$ cm^{-1} (or the near-to-dirty limit). This is shown in Fig. 7 for both compounds. We would like to point out that this value for the impurity parameter is also consistent with that deduced both from the resistivity[12] and the normal state fit to the optical data (see Table I) described in Sec III A, in that the effective γ_D which would enter the Drude formula is $1/[\tau(1+\lambda)]$. Note that the midinfrared band seen in the experimental data cancels out in the conductivity ratio implying that it is not associated with the superconducting state. Our calculations deal with the free carriers only and do not include a midinfrared band contribution.

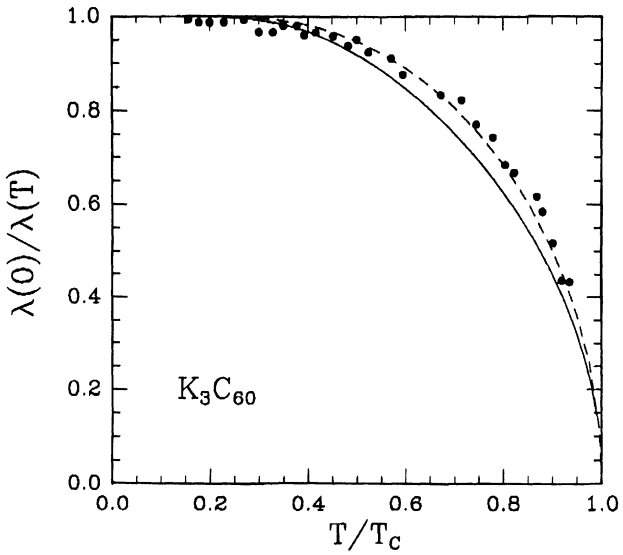

FIG. 11. The inverse temperature-dependent penetration depth normalized to its $T=0$ K value, $\lambda(0)/\lambda(T)$ versus T/T_c. The data is taken from Uemura *et al.* (Ref. 42). The solid curve is the weak-coupling BCS prediction and the dashed curve is the calculation based on the model presented in the text.

In Fig. 10, we display the temperature-dependent resistivity of Fig. 1 normalized to its value at $T=300$ K so as to emphasize the temperature dependence and eliminate the material parameter plasma frequency ω_p. We have also subtracted off the residual resistivity at $T=T_c$ in this plot. The absolute magnitude of the resistivity data could be argued to be not well established in this measurement and so it is more useful to remain with the normalized quantity. We find that the simple phonon spectrum shown in Fig. 9 is able to describe the temperature dependence of the resistivity. This is important to note as the high-T_c oxides have an anomalous linear resistivity which rules out phonons as the dominant pairing mechanism. Including a typical value for the plasma frequency, we find that the absolute value of the calculated resistivity is below that of the data, however, as noted above, the absolute value of the data may not be well established.

In order to complete our complement of optical properties, we present in Fig. 11 the penetration depth also calculated in the same model with the same impurity parameter used to fit the frequency-dependent optical conductivity data. It is found that the data can be well explained by this calculation and that the deviation from the BCS weak-coupling temperature dependence can be explained by impurity scattering, consistent with optical data, and that one does not need to resort to strong-coupling arguments as was done by Mazin *et al.*[60] Thus, it would appear that a self-consistent picture of all the optical properties of the K- and Rb-doped fullerenes presented here can be explained within conventional electron-phonon theory with coupling to high-energy phonons of the intramolecular type. However, we have noted that the gap feature seen in the superconducting phase does not show the expected temperature dependence. In the model discussed here, this gap would close with a temperature dependence similar to the BCS weak-coupling gap but no such shift in the peak in R_s/R_n is seen in the data (see Fig. 8). This remains as an outstanding problem within the present interpretation.

Finally to conclude this section, we would like to briefly point out that we investigated the role of low-frequency intermolecular or librational modes.[61] By introducing a peak in the $\alpha^2F(\omega)$ spectrum at very low frequency, we found that we could not have significant coupling to these modes and explain the data at the same time. The low-frequency modes produce strong-coupling effects and therefore increase the gap ratio to order >4, which is much greater than what is observed in the experimental data. In addition, ignoring that issue and still trying to fit the normalized conductivity, it was not possible to find a value of the impurity parameter which would

provide a good fit to the data. For clean to nearly dirty values of $1/\tau$, the theoretical optical conductivity displayed large Holstein structure in stark disagreement with the data and for $1/\tau$ approaching the dirty limit, the Holstein structure damped down but the theoretical conductivity ratio was always below the experimental data following more closely the Mattis-Bardeen curve. Therefore, we definitely conclude that the experimental data do not support coupling to very low-energy phonon modes for the pairing mechanism in the doped fullerenes.

IV. CONCLUSION

We have reported on our optical investigations on the alkali-doped K_3C_{60} and Rb_3C_{60} superconductors in a broad frequency range. We have discussed the high-frequency part of the excitation spectrum above T_c in terms of interband transitions. Those excitations were found to be in agreement with high-energy electron spectroscopy results and, as well, band-structure calculations.[19,20] At lower frequencies, we have observed a Drude contribution and a fairly broad excitation in the mid-IR. On the other hand, the electrodynamic response of the superconducting ground state is in full agreement with that of a BCS singlet superconductor, and the magnitude of the single-particle gaps also agrees with the weak-coupling limit. Furthermore, beyond the standard BCS approach, we have applied the more complete and sophisticated conventional Eliashberg electron-phonon theory of superconductivity. We have found evidence for a pairing mechanism mainly involving high-frequency intramolecular modes, hence supporting the conclusions based on the BCS theory.

However, the optical conductivity above T_c provides an interesting contrast to the apparently conventional superconducting one. We would like now to briefly discuss the optical superconducting-state properties in the perspective of the unconventional normal-state ones. In fact, while FIR investigations and several other experimental results below T_c are in accord with a BCS weak-coupling limit, the normal state $\sigma_1(\nu)$ on the other hand appears to be very different from that expected from ordinary band theory with weak coupling. The fairly large transfer of spectral weight from the low-frequency Drude-like response to the mid-IR absorption is instead indicative of strong renormalizations in the normal state. This might be the consequence of the important role played by correlation effects. Within the phenomenological two-component picture we found a relevant enhancement of the charge carriers effective mass. Of course, "heavy" quasiparticles should scatter with low-frequency phonons, suggesting a strong-coupling limit of the pairing mechanism in the superconducting state. In this respect, we remark on the similarity between the alkali-doped superconducting fullerenes and the bulk superconductor $Ba_{1-x}K_xBiO_3$ ($x=0.4$ and $T_c=31$ K), where, however, the persistence of short-range charge-density-wave-like order into the superconducting regime has been proposed.[62] In view of these controversial arguments favoring either the weak- or the strong-coupling limit, it is also interesting to recall once again the analysis of the temperature dependence of the resistivity $\rho(T)$.[12,14] As already remarked, at a first glance the functional form $\rho(T)=a+bT^2$ seems to be appropriate but it has been shown that the thermal-expansion corrections decrease the quality of the fit.[63] Of course, a T^2 dependence would be of relevance for an electron-electron scattering mechanism. In relation to this, it is worth noting that, while the size of the isotope effect lends further support to a model of superconductivity involving pairing via high-frequency phonons, sizable corrections from the electron-electron interactions were found to be equally important.[36] Nonetheless, we have shown (see Sec. III C) that a better description of $\rho(T)$ is achieved by analyzing the experimental data from the point of view of the electron-phonon coupling. Similar to our theoretical results, Crespi *et al.* also showed that conventional electron-phonon couplings would be sufficient to account for the superconductivity; with contributions to the coupling from both high- and low-frequency modes. However, the coupling strength to lower-frequency modes (the ones which are relevant for the strong coupling) does not contribute significantly to either the superconducting transition temperature or the gap ratio.[63] Thus, the reconciliation of these apparently disparate aspects may be quite crucial to completely understanding fullerene materials.

ACKNOWLEDGMENTS

The authors are grateful to J. P. Carbotte, M. J. Rice, T. M. Rice, Z. Schlesinger, and D. B. Tanner for fruitful discussions, to S. Cho for sample characterization and to J. Müller and H. P. Staub for technical assistance. One of us (L.D.) wishes to acknowledge the financial support of the Swiss National Foundation for the Scientific Research. The work at UCLA was supported by the Defense Advanced Research Projects Agency through a grant monitored by the Army Research Office and at UCSB by the Natural Sciences and Engineering Research Council of Canada (NSERC).

*Present address: Department of Physics at MIT, Cambridge, MA 02139.

[1] A. F. Hebbard, M. J. Rosseinsky, R. C. Haddon, D. W. Murphy, S. H. Glarum, T. T. M. Palstra, A. P. Ramirez, and A. R. Kortan, Nature (London) **350**, 320 (1991).

[2] K. Holczer, O. Klein, S.-M. Huang, R. B. Kaner, K.-J. Fu, R. L. Whetten, and F. N. Diederich, Science **252**, 600 (1991).

[3] S. Chakraverty and S. Kivelson, Europhys. Lett. **16**, 751 (1991).

[4] C. M. Varma, J. Zaanen, and K. Raghavachari, Science **254**, 989 (1991).

[5]M. Schluter, M. Lannoo, M. Needels, G. A. Baraff, and D. Tomanek, Phys. Rev. Lett. **68**, 526 (1992).
[6]F. C. Zhang, M. Ogata, and T. M. Rice, Phys. Rev. Lett. **67**, 3452 (1991).
[7]Z. Zhang, C.-C. Chen, S. P. Kelty, H. Dai, and C. M. Lieber, Nature (London) **353**, 333 (1991).
[8]L. D. Rotter, Z. Schlesinger, J. P. Cauley, N. Courtel, J. E. Fischer, and A. B. Smith, Nature (London) **355**, 532 (1992).
[9]S. A. Fitzgerald, S. C. Kaplan, A. Rosenberg, A. J. Sievers, and R. A. S. McMordie, Phys. Rev. B **45**, 10 165 (1992).
[10]L. Degiorgi, G. Grüner, P. Wachter, S.-M. Huang, J. Wiley, R. L. Whetten, R. B. Kaner, K. Holczer, and F. Diederich, Phys. Rev. B **46**, 11 250 (1992).
[11]L. Degiorgi, P. Wachter, G. Grüner, S.-M. Huang, J. Wiley, and R. B. Kaner, Phys. Rev. Lett. **69**, 2987 (1992).
[12]O. Klein, G. Grüner, S.-M. Huang, J. B. Wiley, and R. B. Kaner, Phys. Rev. B **46**, 11 247 (1992).
[13]T. T. M. Palstra, R. C. Haddon, A. F. Hebbard, and J. Zaanen, Phys. Rev. Lett. **68**, 1054 (1991).
[14]X. D. Xiang, J. G. Hou, G. Briceno, W. A. Vareka, R. Mostrovoy, A. Zettl, V. H. Crespi, and M. L. Cohen, Science **256**, 1190 (1992).
[15]Y. Iwasa, K. Tanaka, T. Yasuda, T. Koda, and S. Koda, Phys. Rev. Lett. **69**, 2284 (1992).
[16]D. B. Tanner and T. Timusk, in *Physical Properties of High-Temperature Superconductors III,* edited by D. M. Ginsberg (World Scientific, Singapore, 1992), p. 363.
[17]S. Tajima, S. Uchida, M. Masaki, H. Takagi, K. Kitazawa, and S. Tanaka, Phys. Rev. B **32**, 6302 (1985).
[18]L. I. Buravov, A. V. Zvarykina, N. D. Kushch, V. N. Lankhin, V. A. Merzhanov, A. G. Khomenko, and E. B. Yagubskii, Zh. Eksp. Teor. Fiz. **95**, 3 (1989) [Sov. Phys. JETP **68**, 1 (1989)].
[19]Y.-N. Xu, M.-Z. Huang, and W. Y. Ching, Phys. Rev. B **44**, 13 171 (1991).
[20]E. Sohmen, J. Fink, and W. Kraetschmer, Z. Phys. B **86**, 87 (1992).
[21]W. H. Wong, M. Hanson, W. G. Clark, K. Holczer, G. Grüner, J. D. Thompson, R. L. Whetten, S.-M. Huang, R. B. Kaner, and F. Diederich, Europhys. Lett. **18**, 79 (1992).
[22]S. C. Erwin and W. E. Pickett, Science **254**, 842 (1991).
[23]R. Tycko, G. Dabbagh, M. J. Rosseinsky, D. W. Murphy, A. P. Ramirez, and R. M. Fleming, Phys. Rev. Lett. **68**, 1912 (1992).
[24]T. Takahashi, S. Suzuki, T. Morikawa, H. Katayama-Yoshida, S. H. Asegawa, H. Inokuchi, K. Seki, K. Kikuchi, S. Suzuki, K. Ikemoto, and Y. Achiba, Phys. Rev. Lett. **68**, 1232 (1992).
[25]B. Batlogg, Physica B **126**, 275 (1984).
[26]M. Merkel, M. Knupfer, M. S. Golden, J. Fink, R. Seemann, and R. L. Johnson, Phys. Rev. B **47**, 11 470 (1993).
[27]M. J. Rice and H.-Y. Choi, Phys. Rev. B **45**, 10 173 (1992).
[28]M. J. Rice, Phys. Rev. Lett. **37**, 36 (1976).
[29]T. Pichler, M. Matus, and H. Kuzmany, Solid State Commun. **86**, 221 (1993).
[30]M. C. Martin, D. Koller, and L. Mihaly, Phys. Rev. B **47**, 14 607 (1993).
[31]C. E. Johnson, H. W. Jiang, K. Holczer, R. B. Kaner, R. L. Whetten, and F. Diederich, Phys. Rev. B **46**, 5880 (1992).
[32]M. P. Gelfand and J. P. Lu, Phys. Rev. Lett. **68**, 1050 (1992).
[33]M. P. Gelfand and J. P. Lu, Phys. Rev. B **46**, 4367 (1992).
[34]M. P. Gelfand and J. P. Lu, Appl. Phys. A **53**, 215 (1993).
[35]A. I. Liechtenstein, I. I. Mazin, O. Gunnarsson, O. K. Andersen, V. P. Antropov, and S. E. Burkov (unpublished).
[36]A. P. Ramirez, A. R. Kortan, M. J. Rosseinsky, S. J. Duclos, A. M. Mujsce, R. C. Haddon, D. W. Murphy, A. V. Makhija, S. M. Zahurak, and K. B. Lyons, Phys. Rev. Lett. **68**, 1058 (1992).
[37]A. P. Ramirez, M. J. Rosseinsky, D. W. Murphy, and R. C. Haddon, Phys. Rev. Lett. **69**, 1687 (1992).
[38]G. Quirion, C. Bourbonnais, E. Barthel, P. Auban, D. Jerome, J. M. Lambert, A. Zahab, P. Bernier, C. Fabre, and A. Rassat, Europhys. Lett. **21**, 233 (1993).
[39]R. F. Kiefl, W. A. MacFarlane, K. H. Chow, S. Dunsiger, T. L. Duty, T. M. S. Johnston, J. W. Schneider, J. Sonier, L. Brard, R. M. Strongin, J. E. Fischer, and A. B. Smith III, Phys. Rev. Lett. **70**, 3987 (1993).
[40]See, for example, M. Tinkham, in *Introduction to Superconductivity,* edited by R. E. Krieger (McGraw-Hill, New York, 1975).
[41]This frequency is 350 cm^{-1} for K_3C_{60} and for Rb_3C_{60}.
[42]Y. J. Uemura, A. Keren, L. P. Le, G. M. Luke, B. J. Sternlieb, W. D. Wu, J. H. Brewer, R. L. Whetten, S.-M. Huang, S. Liu, R. B. Kaner, F. Diederich, S. Donovan, G. Grüner, and K. Holczer, Nature (London) **352**, 605 (1991).
[43]Y. T. Uemura, L. P. Le, and G. M. Luke, *Proceedings of the International Conference on Science and Technology of Synthetic Metals, Goeteborg, Sweden, 1992* [Synth. Met. **56**, 2845 (1993)].
[44]D. C. Mattis and J. Bardeen, Phys. Rev. **111**, 412 (1958).
[45]H.-Y. Choi and M. J. Rice (unpublished).
[46]J. P. Carbotte, Rev. Mod. Phys. **62**, 1027 (1990).
[47]W. Shaw and J. C. Swihart, Phys. Rev. Lett. **20**, 1000 (1968).
[48]S. B. Nam, Phys. Rev. **156**, 470 (1967).
[49]S. B. Nam, Phys. Rev. **156**, 487 (1967).
[50]P. B. Allen, Phys. Rev. **B3**, 305 (1971).
[51]E. J. Nicol (unpublished).
[52]W. Lee, D. Rainer, and W. Zimmermann, Physica C **159**, 535 (1989).
[53]N. E. Bickers, D. J. Scalapino, R. T. Collins, and Z. Schlesinger, Phys. Rev. B **42**, 67 (1990).
[54]G. Grimvall, *The Electron-Phonon Interaction in Metals* (North-Holland, Amsterdam, 1981).
[55]J. M. Daams and J. P. Carbotte, J. Low Temp. Phys. **43**, 263 (1981).
[56]D. Rainer and G. Bergmann, J. Low Temp. Phys. **14**, 501 (1974).
[57]P. B. Allen and B. Mitrovic, in *Solid State Physics: Advances in Research and Applications,* edited by H. Ehrenreich (Academic, New York, 1982), Vol. 37, p. 1.
[58]O. Gunnarsson and G. Zwicknagl, Phys. Rev. Lett. **69**, 957 (1992).
[59]B. Hayman and J. P. Carbotte, Can. J. Phys. **49**, 1952 (1971); J. Phys. F **1**, 828 (1971).
[60]I. I. Mazin, O. V. Dolgov, A. Golubov, and S. V. Shulga, Phys. Rev. B **47**, 538 (1993).
[61]E. J. Nicol, Physica B (to be published).
[62]S. H. Blanton, R. T. Collins, K. H. Kelleher, L. D. Rotter, and Z. Schlesinger, Phys. Rev. B **47**, 996 (1993).
[63]V. H. Crespi, J. G. Hou, X.-D. Xiang, M. L. Cohen, and A. Zettl, Phys. Rev. B **46**, 12 064 (1992).